000871

SC 1004-A (3-55)

UNCLASSIFIED

SANDIA SYSTEMATIC DECLASSIFICATION REVIEW
DOE CLASSIFICATION STAMP
CLASSIFICATION CHANGED TO: U
CLASSIFIED BY: W. C. Layne
Emelda Selph 10-24-96
R. T. Duff 10/29/96
PERSON VERIFYING MARKING & DATE
CLASSIFIED BY: 97SN019
DATED: 10-22-96

[redacted]

Ref. Sym: 7223(527)

[redacted]

INVENTORIED

MAR 8 1965

3427-1

SCTM 198-58-51

AERODYNAMIC HEATING OF THE XMC-903 RADOME

S. McAlees, Jr. - 5144
R. J. Loncharich - 5144

SANDIA SYSTEMATIC DECLASSIFICATION REVIEW
1st Review Date: 7-30-79
Authority: ☐ ADC ☒ ADD
Name: CCRP-RR
2nd Review Date: 10-22-96
Authority: ADC
Name: W Layne
Determination (Circle Numbers):
1 Classification Retained
2 Classification Changed to: U
3 Contains No DOE Classified Information
4 Coordinate With:
5 Contains UCAI?
6 Comments:

[redacted]

ABSTRACT

The stagnation temperature and temperature rise of the XMC-903 radome at nine stations along the body have been computed on the REAC. Results were obtained from the solution of the heat balance equations for heat inputs generated during external carriage of the weapon through the proposed delivery schedule. The analysis shows that the XMC-903 radome is capable of withstanding the imposed thermal environment.

[redacted]

Case No. 409.43 [redacted] April 28, 1958

[redacted]

UNCLASSIFIED

THIS DOCUMENT CONSISTS OF 31 PAGE(S)
NO 32 OF 32 COPIES, SERIES A

UNCLASSIFIED

[redacted]

Ref. Sym: 7223(527)

DISTRIBUTION:

1/32A - E. H. Draper, 1200
2/32A - L. A. Hopkins, Jr., 1400
3/32A - B. S. Biggs, 1600
4/32A - S. C. Hight, 5100
5/32A - R. A. Bice, 5200
6/32A - W. J. Howard, 8100
7/32A - J. P. Cody, 1220
8/32A - D. R. Cotter, 1240
9/32A - G. E. Hansche, 5130
10/32A - A. Y. Pope, 5140
11/32A - W. E. Treibel, 1246
12/32A - C. R. Carlson, 1261
13/32A - D. M. Bruce, 1282
14/32A - J. W. McKiernan, 1283
15/32A - A. J. Roth, 1422
16/32A - W. D. Stoppkotte, 1422
17/32A - P. Syroid, 1613
18/32A - P. W. Rowe, 5141
19/32A - R. C. Maydew, 5142
20/32A - K. C. Crowder, 5143
21/32A - W. H. Curry, 5144
22/32A - S. McAlees, Jr., 5144
23/32A - R. J. Loncharich, 5144
24/32A - J. R. Piper, 1246-2
25/32A - J. McMinn, 8221
26/32A - R. K. Smeltzer, Central File Record, 7221
27-32/32A - L. F. Parman, 7223

1/1B - 9320

UNCLASSIFIED

[redacted]

SUMMARY

The results of an analytical investigation of the effects of aerodynamic heating on the XMC-903 radome (fig. 1) are presented. The analysis shows that the maximum radome temperature attained during the proposed external carriage of the weapon is 213°F which is well within the temperature limitations of all structural materials used in the radome design. It is concluded that the XMC-903 radome is thermally compatible with the intended flight plan and resulting thermal environment.

UNCLASSIFIED

[redacted]

UNCLASSIFIED

INTRODUCTION

The stagnation temperature and temperature rise at nine stations over the forward portion of the XMC-903 radome (fig. 1) have been determined for heat inputs derived during the proposed delivery schedule supplied by Division 1422. The proposed delivery schedule for maximum altitude and speed is defined by MC-903 Environmental Criterion, Ref. Sym: 1222-(56) as follows: 500 nautical mile cruise at 0.95 Mach starting at 40,000 feet and ending at 50,000 feet followed by a 127 nautical mile acceleration and climb, ending at Mach 2.0 and 60,000 feet followed by a ten minute dash at Mach 2.0 and 60,000 feet. The flight profile is presented later in the form of altitude and Mach number as a function of time for calculation of instantaneous heat inputs. The specific analysis includes determination of the radome skin temperatures at four stations on the Vibrin # 135 nose, at the three partitions containing "O" rings and "insulation rings" and at two intermediate stations on the thin metal wall structure. Section views of the three partitions are shown in figures 2, 3 and 4. The analysis also includes a study of the temperature distribution over the body at various times during the flight.

The purpose of this report is to determine the maximum temperature attained on the XMC-903 radome during external carriage through the weapon's proposed delivery schedule.

UNCLASSIFIED

[redacted]

UNCLASSIFIED

[redacted]

SYMBOLS

c	Specific heat, $\frac{BTU}{Lb\text{-}°R}$
C_p	Pressure coefficient, $\frac{P_\delta - P_\infty}{0.7\ P_\infty M_\infty^2}$
h	Heat transfer coefficient, $\frac{BTU}{Ft^2\text{-}Sec\text{-}°R}$
k	Thermal conductivity, $\frac{BTU\text{-}Ft}{Ft^2\text{-}Sec\text{-}°R}$
M_∞	Free stream Mach number
M_δ	Mach number at outer edge of boundary layer
N_{ST}	Stanton number, $\frac{h}{\rho Vc}$, (based on local air properties)
P_δ	Pressure at outer edge of boundary layer, $\frac{Lb}{Ft^2}$
P_∞	Free stream pressure, $\frac{Lb}{Ft^2}$
R	Recovery factor, 0.85 for laminar B.L. and 0.90 for turbulent B.L.
T_{aw}	Recovery temperature, °R, $T_{aw} = T_\delta\ (1 + \frac{\gamma-1}{2} RM_\delta^2)$
T_δ	Temperature at outer edge of boundary layer, °R
T_o	Stagnation temperature, °R
T_S	Temperature of skin material, °R
V_δ	Velocity at outer edge of boundary layer, Ft/Sec
x	Radial distance, feet
α	Thermal diffusivity, $\frac{k}{\rho c}$, $\frac{Ft^2}{Sec}$ (based on skin material properties)
θ	Time, seconds
ρ	Density, $\frac{Lb}{Ft^3}$

UNCLASSIFIED

[redacted]

ANALYSIS

The analysis is subject to the following assumptions:

1. Radiation from the outer skin is negligible .
2. There is no longitudinal conduction of heat in the radome outer skin.
3. The inner surface of the radome skin is a perfect insulator.

The assumptions listed here are conservative. The combined effect of these assumptions will result in theoretical skin temperatures higher than those actually attained during external carriage of the radome.

The general heat balance equations at a point on the radome may be expressed as

$$\frac{\partial T}{\partial \theta} = \alpha \frac{\partial^2 T}{\partial x^2} \tag{1}$$

with the initial condition (explained below):

$$T_{(x,0)} = T_{aw} \tag{2}$$

and the boundary conditions:

$$-k \left.\frac{\partial T}{\partial x}\right| = h_{(\theta)} \left[T_{aw}(\theta) - T_s(\theta) \right] \tag{3}$$

x = outer surface

$$-k \left.\frac{\partial T}{\partial x}\right| = 0 \tag{4}$$

x = inner surface

The initial 500 nautical mile cruise at Mach 0.95 between 40,000 and 50,000 feet requires 55 minutes during which time the boundary layer recovery temperature is constant. Since essentially no heating takes place during this cruise, the cruise time is used only to establish the radome wall temperature equal to the boundary layer recovery temperature.

DISCUSSION

The XMC-903 radome is subjected to external carriage in the Mach range from 1.0 to 2.0 for a period of nine minutes followed by a ten minute period at Mach 2.0 during the proposed delivery schedule for the weapon. As the result of aerodynamic shape, materials, and construction used in the design of the radome, different temperature-time response curves are obtained at various stations along the body length. Since the materials used in the radome construction have temperature capabilities of approximately 600°F, it is desirable to know the maximum temperature of the materials attained as a result of the imposed thermal environment. The imposed thermal environment was derived from the proposed flight program which is shown graphically in the form of Mach number and altitude as a function of time in figure 5. Since no heating takes place during the first 55 minutes of the flight due to the low Mach number and high altitude, this portion of the flight was used only to establish initial skin temperatures equal to the boundary layer recovery temperature. Heat inputs were derived for the remaining 19 minutes of the proposed delivery schedule. The stagnation temperature and boundary layer recovery temperatures resulting from the flight profile for the laminar and turbulent boundary layers are shown in figure 6. In order to establish the heat transfer to the body, the local heat transfer coefficient distribution over the body was determined from local flow conditions at each body station in question. Pressure coefficient distribution (fig. 7) and Stanton number distribution (fig. 8) over the body were obtained from references 1, 2, 3, and from unpublished Sandia wind tunnel test results for similarly shaped bodies and appropriate flight conditions. The local static pressure distribution over the body was determined directly from the pressure coefficient distribution while the total pressure over the body was assumed equal to the total pressure behind a normal shock wave up to station 6.875. Isentropic expansion over the body behind the shock was assumed in this region. Aft of body

station 12.0 it was assumed that the total pressure had returned to the free stream value. A ratio of static to total pressure on the body is sufficient for determination of local Mach number and subsequent evaluation of local flow conditions over the body. The local flow conditions where then applied to the Stanton number distribution for final determination of the heat transfer coefficient as a function of time at the body stations under consideration. Values of the heat transfer coefficient are presented in figures 9 and 10. In evaluating the heat inputs, a laminar boundary layer was assumed to exist up to body station 3.0; a fully developed turbulent layer was assumed aft of body station 6.0. This transition range falls within the limits as presented in reference 1, 2, and 3.

Results indicate that the maximum temperature gradient across the Vibrin #135 nose cone is approximately 16°F. No appreciable gradient was found to exist in the metal walls and metal partitions. Wall temperature variation with flight time is presented for each body station studied in figures 11 through 19. Temperature distributions along the body for various times during the delivery schedule are presented in fig. 20. The pronounced effect of body construction in the form of a heat sink at the three major partitions is evident from the sudden drop in temperature and slower rise time in these regions. The wall thickness at the partitions was taken as 1.0 inch to the insulating ring at body station 6.875, 0.30 inch to the insulating ring at body station 17.5 and 0.90 inch to the "O"-ring at body station 25.5. Since the body stations were considered isolated elements in the skin, the temperature gradient from the thin skin sections into the heat sink is not known and the value shown in fig. 20 is estimated. The exact extent of this interaction region is unimportant since in this analysis the maximum temperature attained in each region is of primary concern. The radome skin temperature at body station 0 was not calculated since the maximum temperature for a blunt body does not occur at the stagnation point. It

is believed that the maximum temperature near the stagnation point occurs near body station 0.5 in this particular problem. It may be observed from fig. 20 that the maximum temperature attained at any body station throughout the flight is 213°F.

CONCLUSIONS

1. The temperature capabilities of the XMC-903 radome are well in excess of the 213°F attained during the proposed delivery schedule of the weapon.

2. Aerodynamic heating inputs may be used in conjunction with inputs generated from internal electronic sources in determining final temperatures of critical components in the XMC-903 radome.

REFERENCES

1. Garland, Benjamine J., and Chauvin, Leo T.: Measurements of Heat Transfer and Boundary-Layer Transition on an 8-inch Diameter Hemisphere Cylinder in Free Flight for a Mach Number Range of 2.00 to 3.88 NACA-RM-L57D04a, 1957.

2. Chauvin, Leo T., and Speegle, Katherine C.: Boundary-Layer-Transition and Heat-Transfer Measurements from Flight Tests of Blunt and Sharp 50° Cones at Mach Numbers from 1.7 to 4.7. NACA-RM-L57D04, 1957.

3. Buglia, James I.: Heat Transfer and Boundary-Layer Transition on a Highly Polished Hemisphere-Cone in Free Flight at Mach Numbers up to 3.14 and Reynolds Numbers up to 24×10^6. NACA-RM-L57D05, 1957.

UNCLASSIFIED

Ref. Sym: 7223(527)

000882

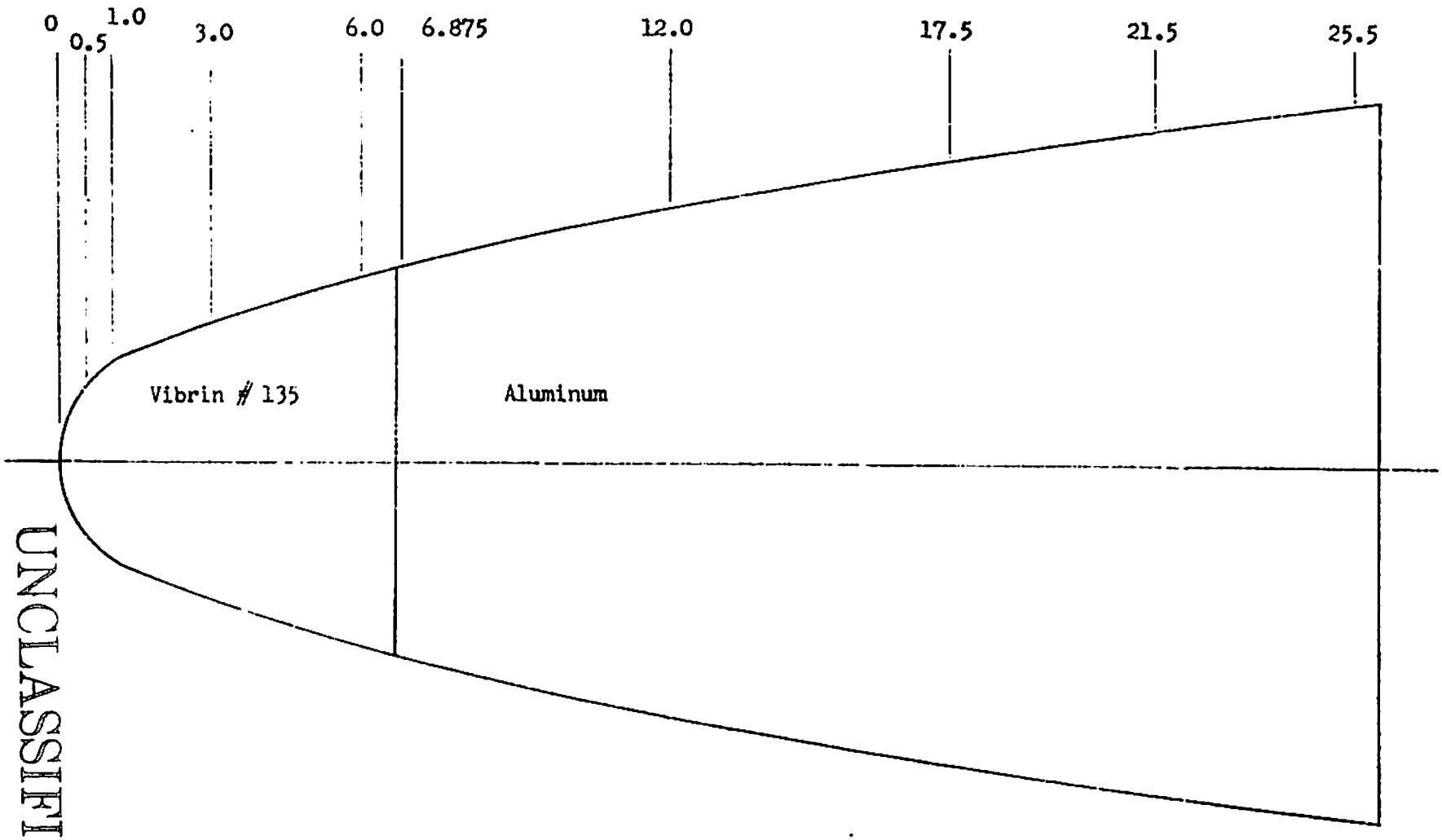

FIG. 1 - SKETCH OF XMC-903 RADOME

UNCLASSIFIED

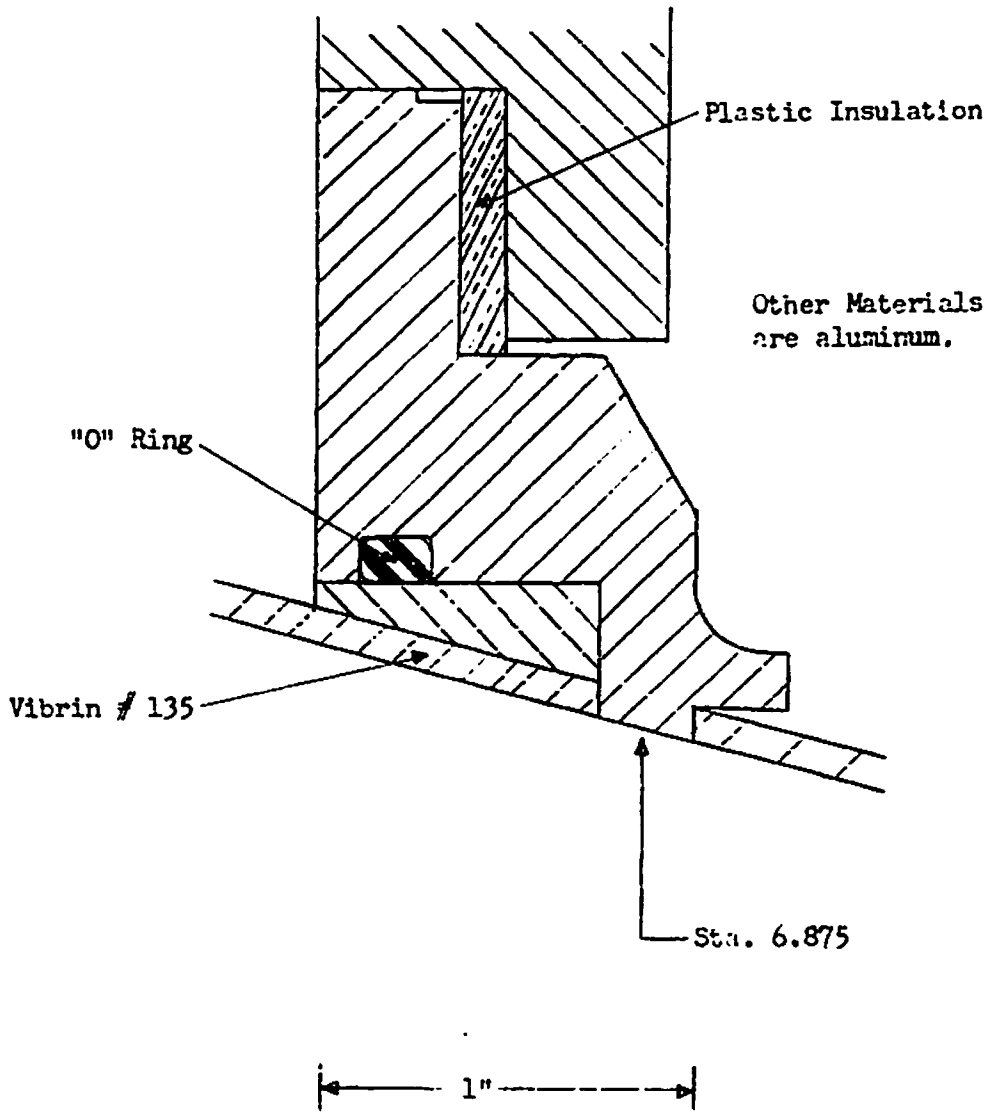

Note: Section views Of Sta. 0.5, 1.0, and 3.0 have been omitted since they consist only of the 0.094 in. Vibrin # 135.

FIG. 2 - SECTION VIEW AT STA. 6.875

Other materials
are aluminum.

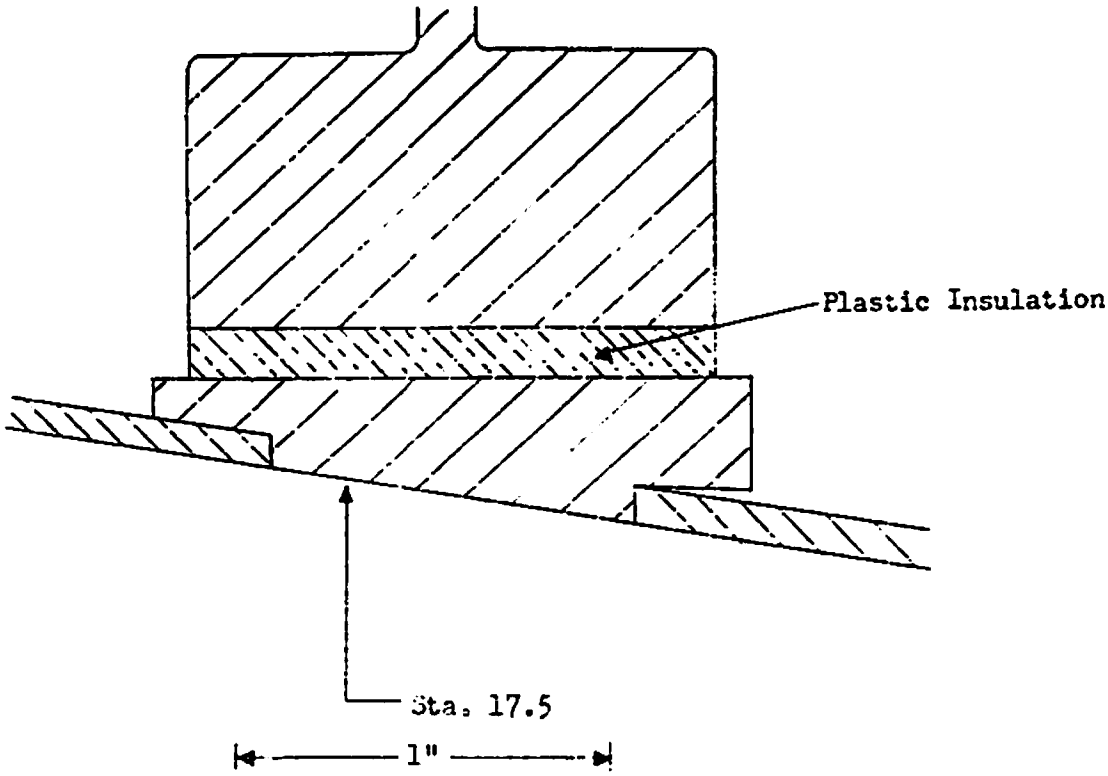

Note: Section views of Sta. 12.0 and 21.5 are omitted since they consist only of the 0.094 in. aluminum.

FIG. 3 - SECTION VIEW AT STA. 17.5

Other materials
are aluminum.

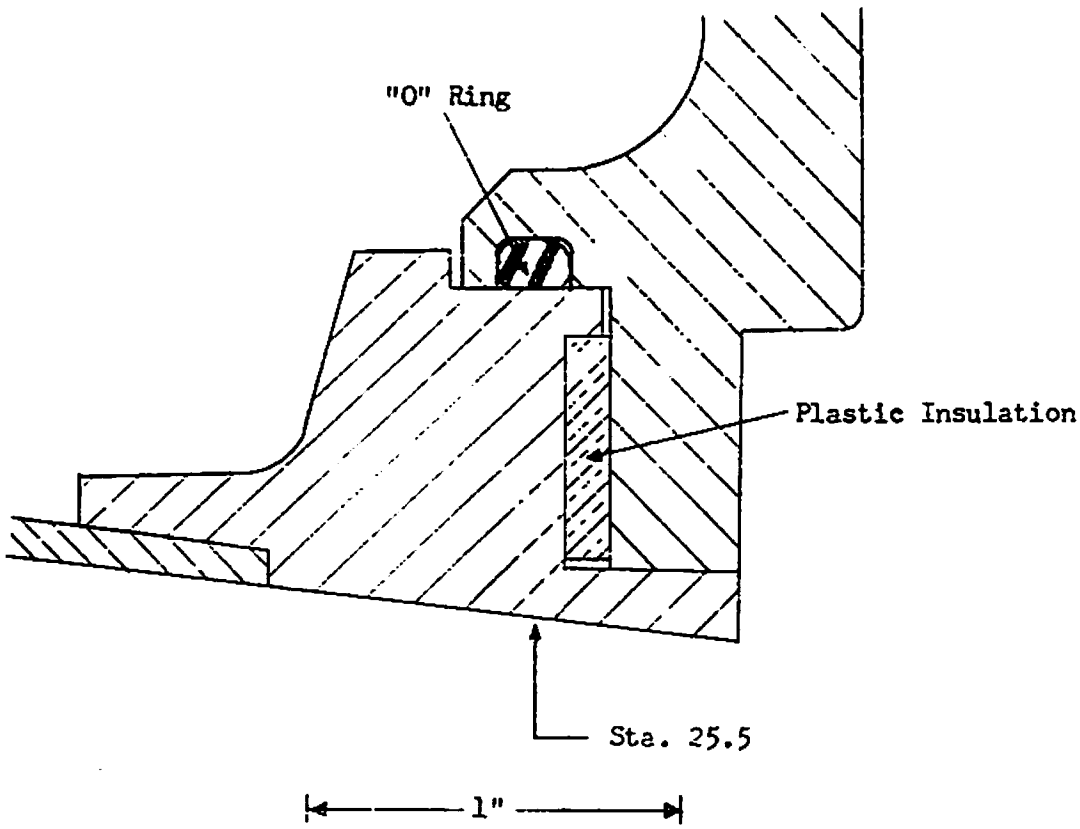

FIG. 4 - SECTION VIEW OF STA. 25.5

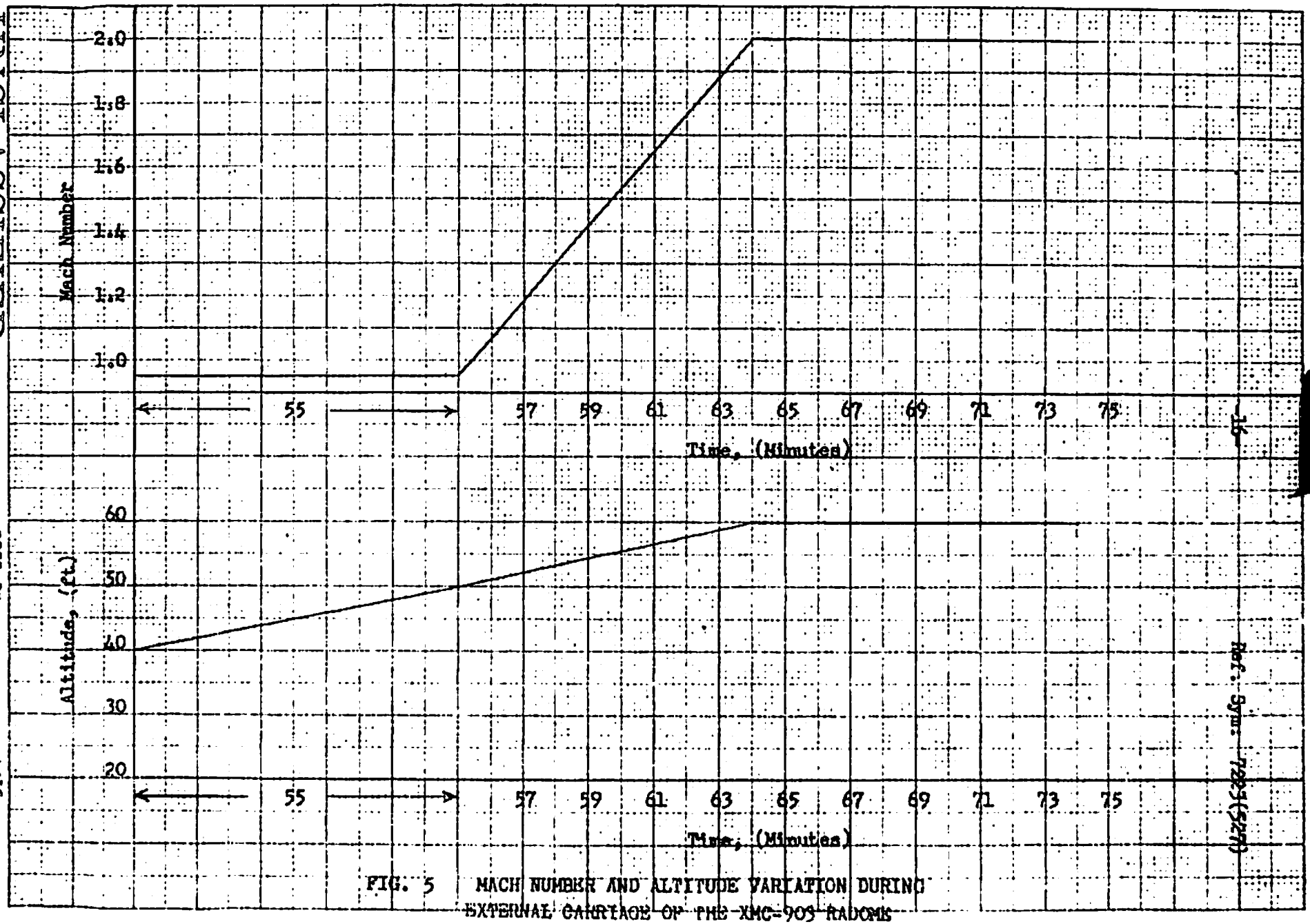

FIG. 5 MACH NUMBER AND ALTITUDE VARIATION DURING EXTERNAL CARRIAGE OF THE XMC-903 RADOME

Ref. Sym. 7223(527)

UNCLASSIFIED
REPORT NO.
SANDIA CORPORATION
ALBUQUERQUE, NEW MEXICO
[redacted]
-17-
000887
PAGE

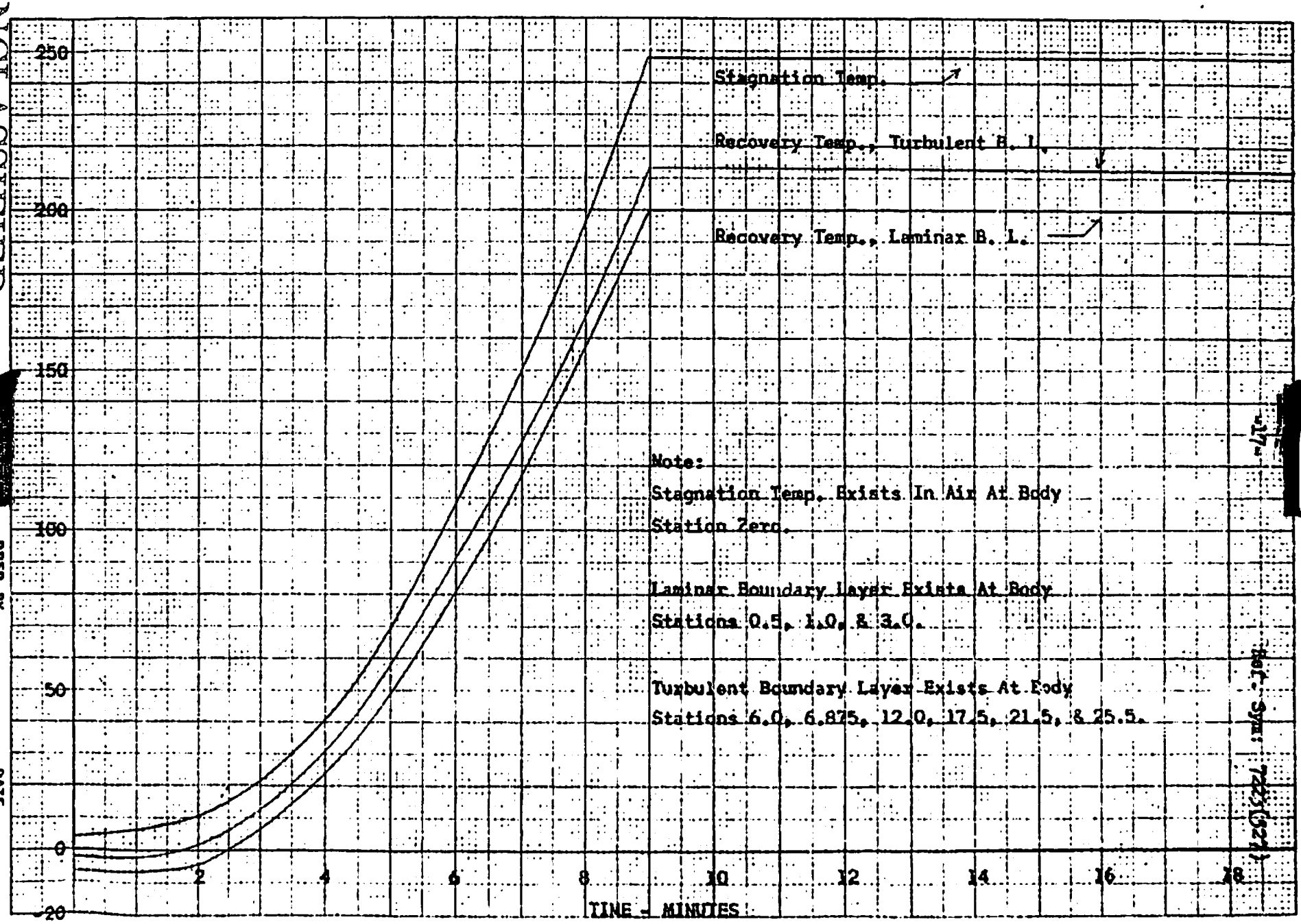

UNCLASSIFIED

SANDIA CORPORATION
ALBUQUERQUE, NEW MEXICO

10 X 10 TO THE ½ INCH 359-11
KEUFFEL & ESSER CO.

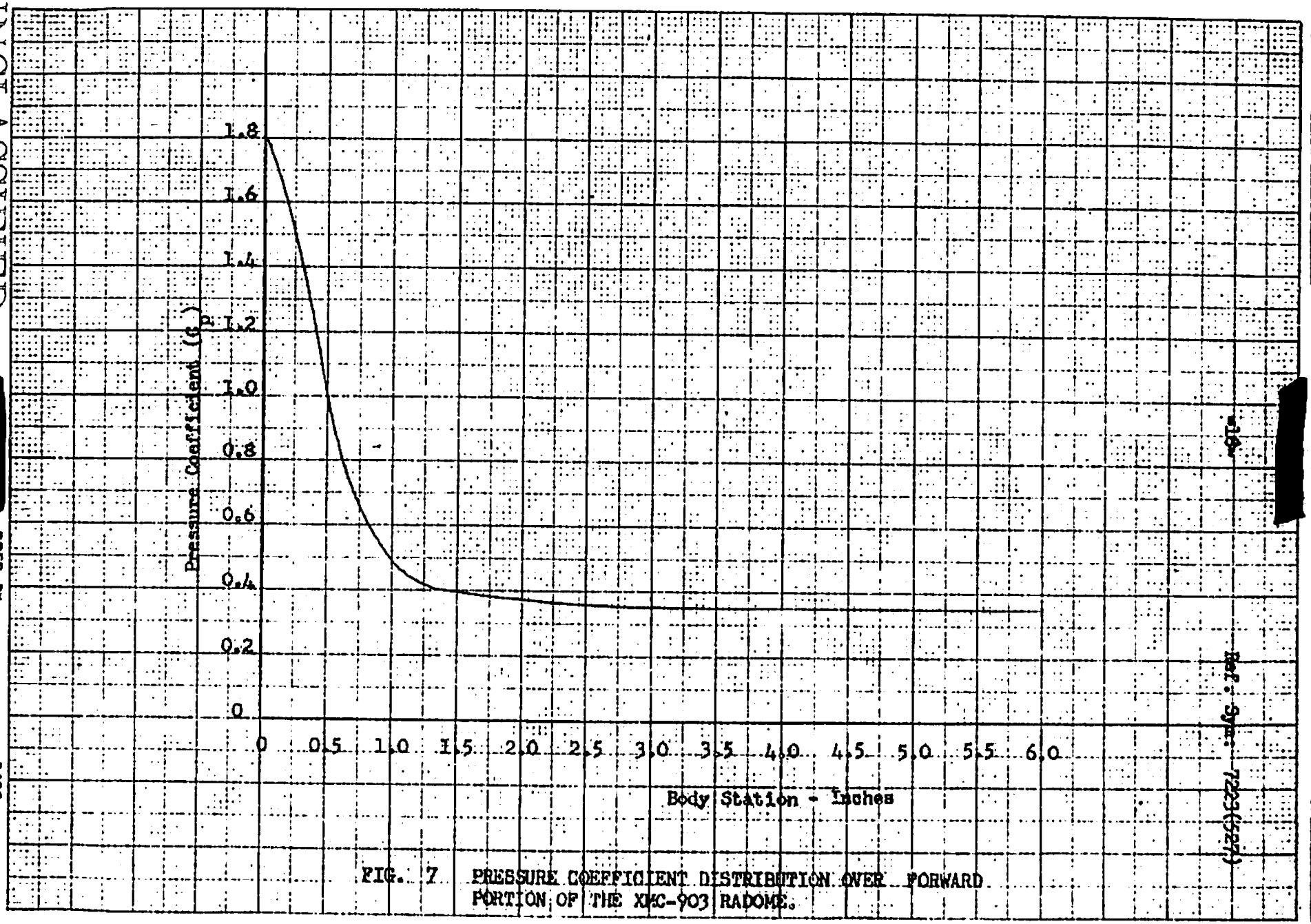

FIG. 7 PRESSURE COEFFICIENT DISTRIBUTION OVER FORWARD PORTION OF THE XMC-903 RADOME.

UNCLASSIFIED

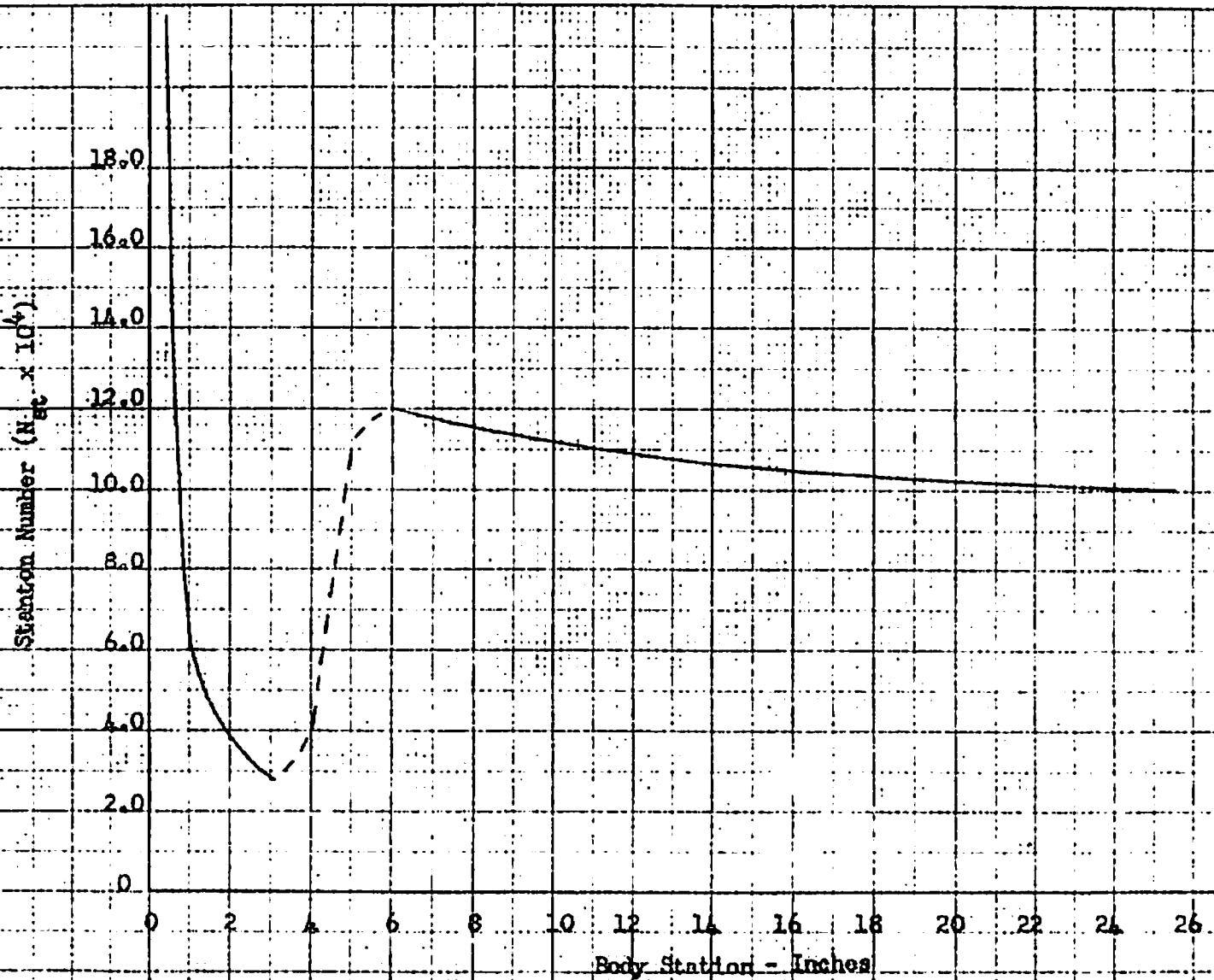

FIG. 8 STANTON NUMBER DISTRIBUTION OVER FORWARD PORTION OF THE XMC-903 RADOME

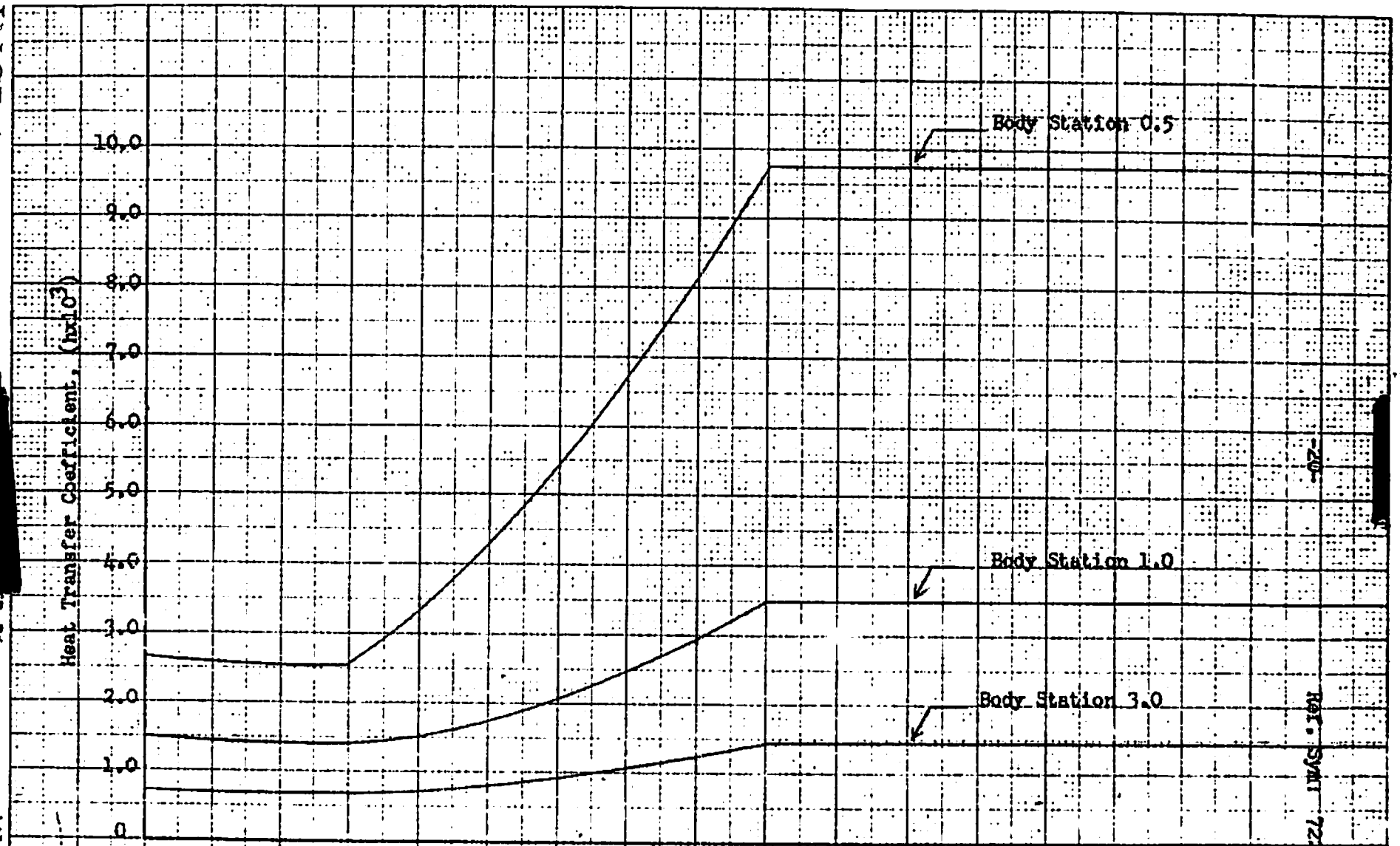

FIG. 9 VARIATION OF HEAT TRANSFER COEFFICIENT DURING EXTERNAL CARRIAGE OF THE XMC-903 RADOME

UNCLASSIFIED

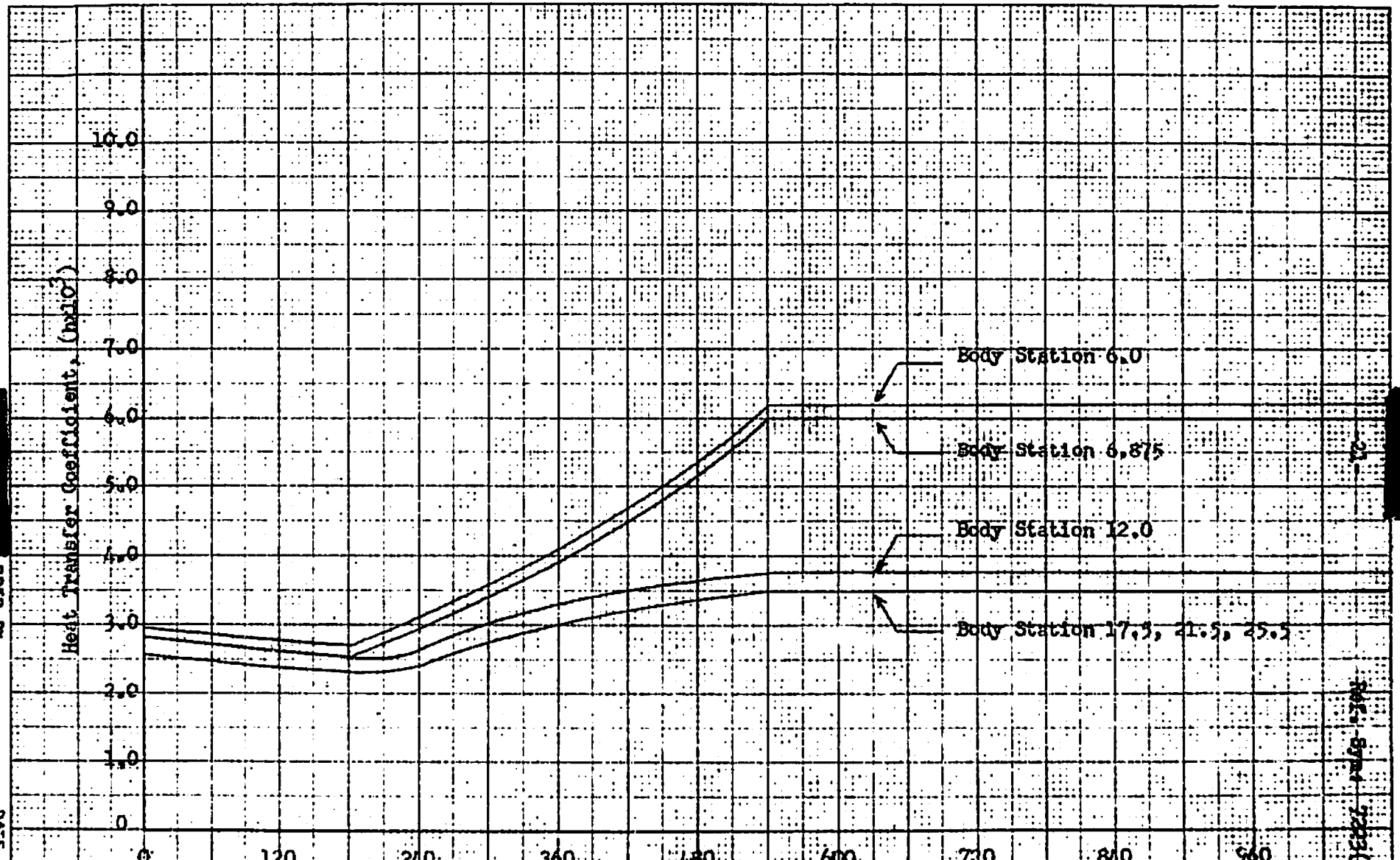

FIG. 10 VARIATION OF HEAT TRANSFER COEFFICIENT DURING EXTERNAL CARRIAGE OF THE XMC-903 RADOME

UNCLASSIFIED

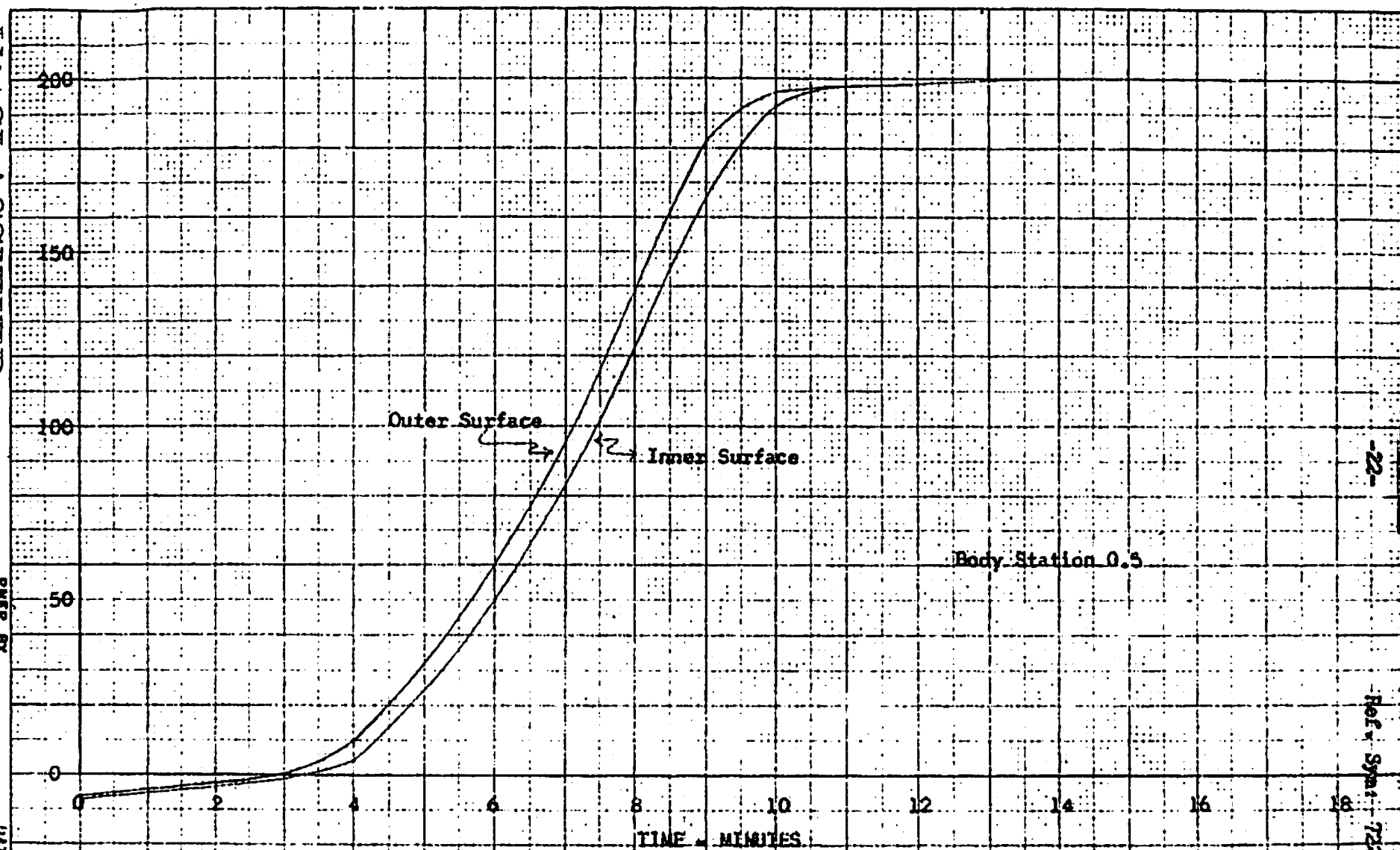

Fig. 11 Temperature - Time Response Resulting From External Carriage Of The XMC-903 Radome.

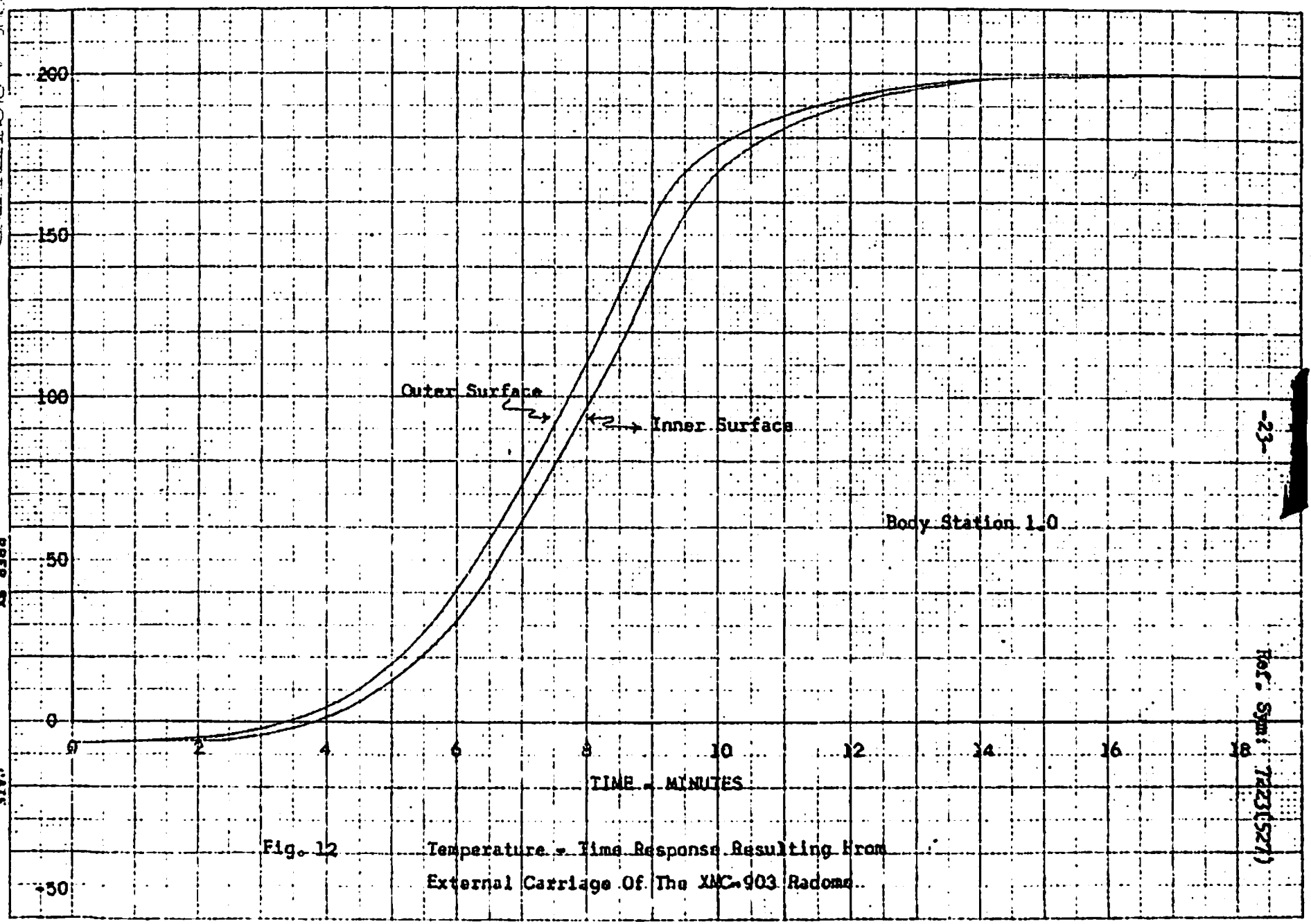

Fig. 12 Temperature - Time Response Resulting From External Carriage Of The XMC-903 Radome

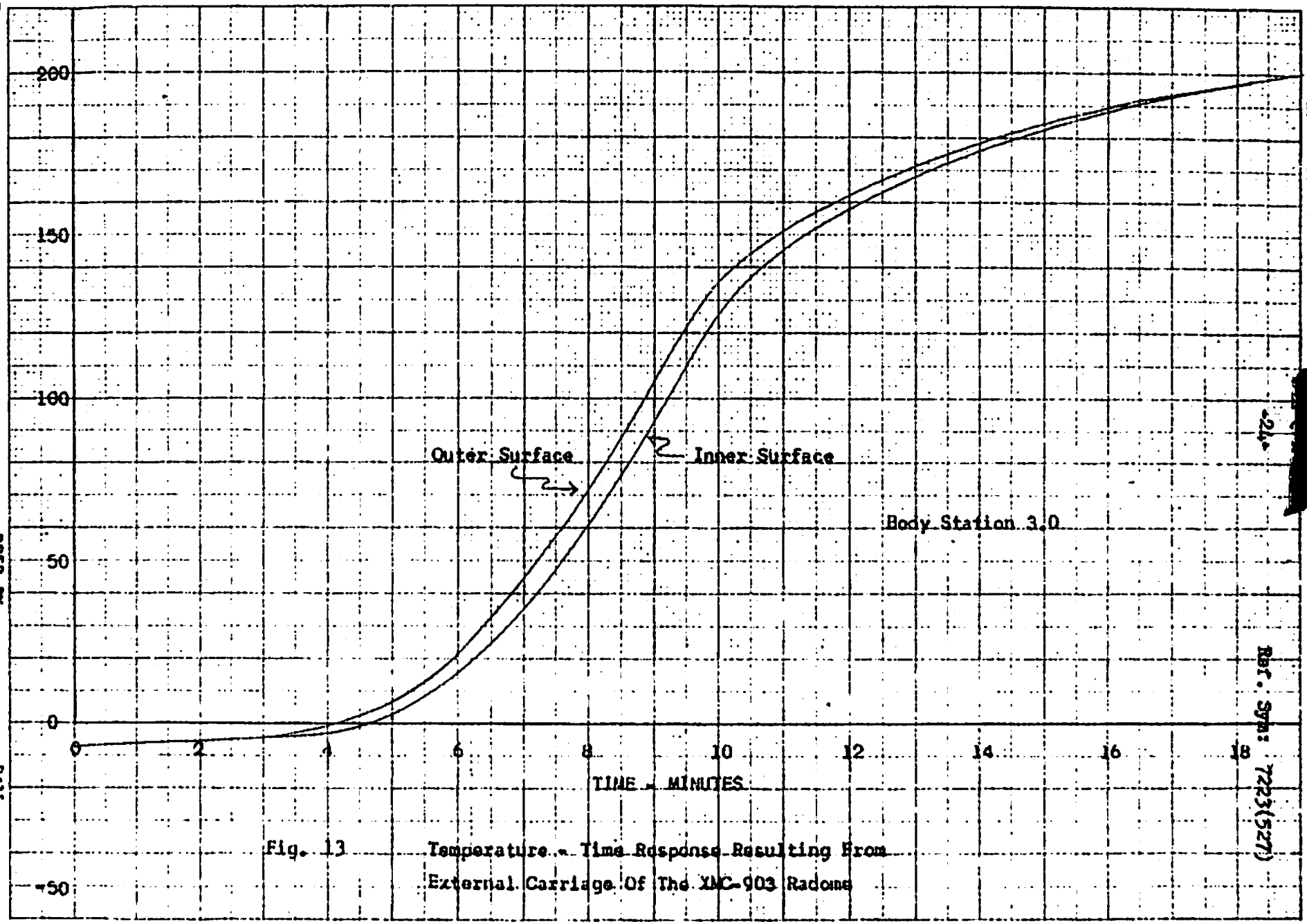

Fig. 13 Temperature - Time Response Resulting From External Carriage Of The XMC-903 Radome

UNCLASSIFIED

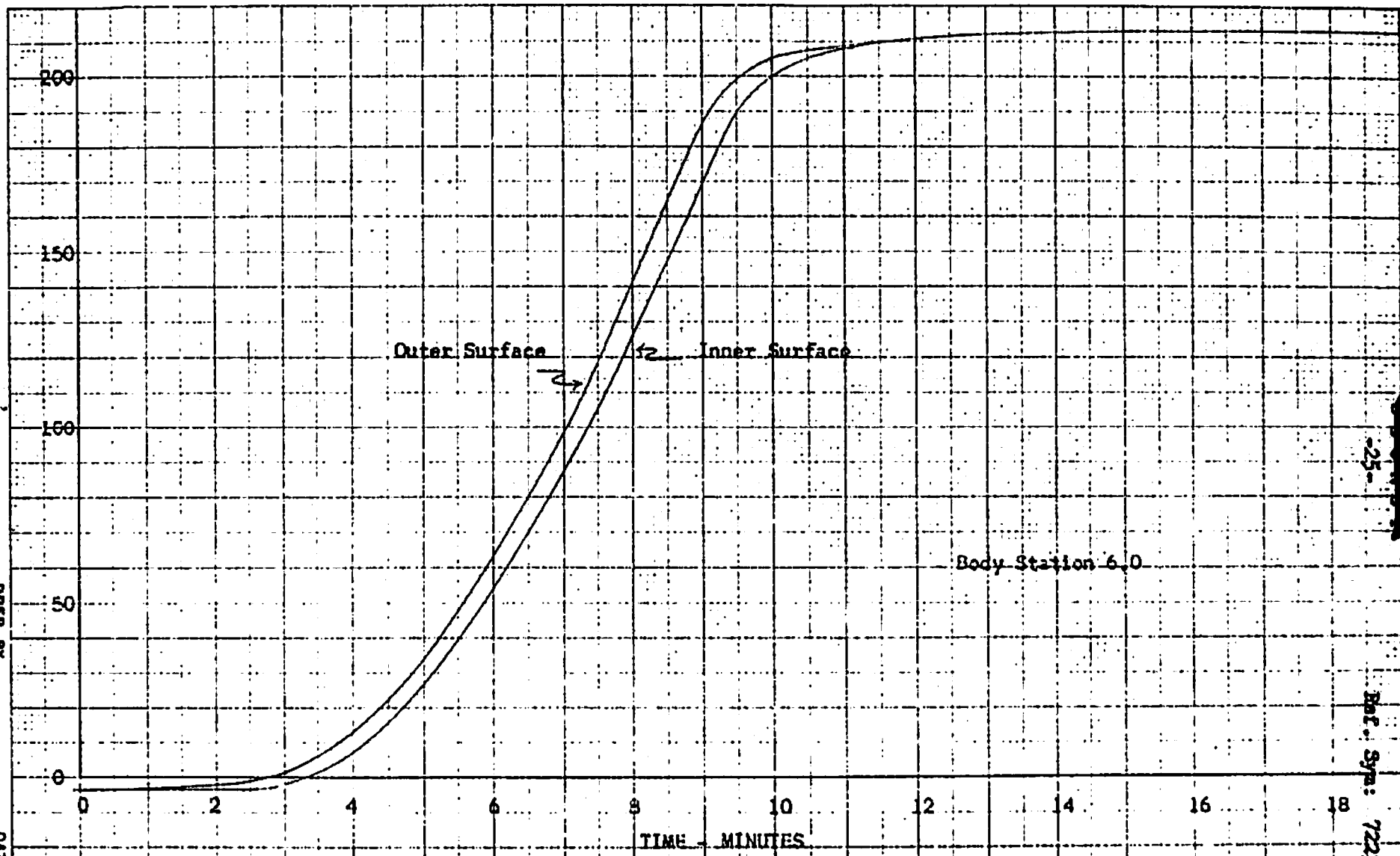

Fig. 14 Temperature - Time Response Resulting From External Carriage Of The XMC-903 Radome

UNCLASSIFIED

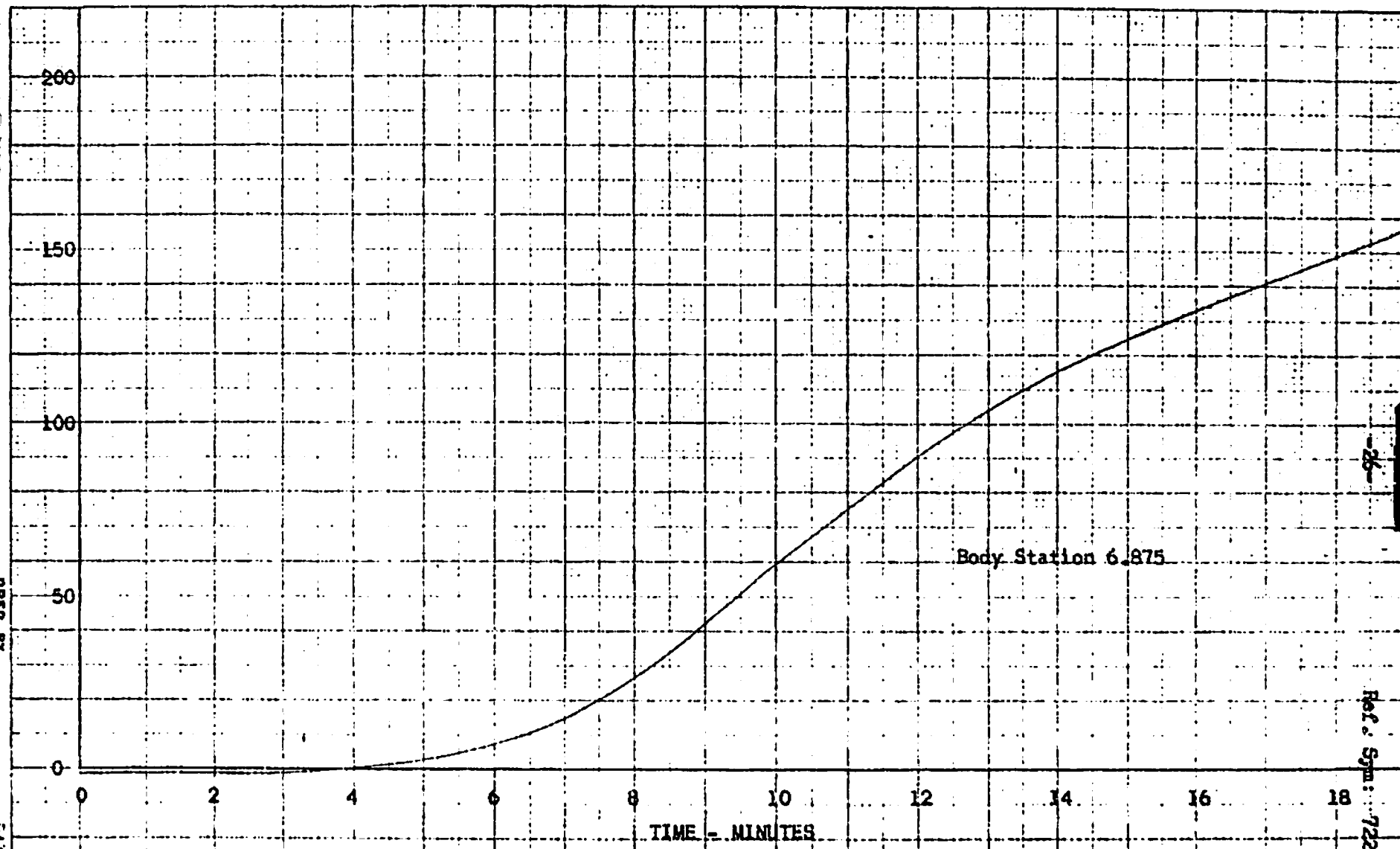

Fig. 15 Temperature - Time Response Resulting From External Carriage Of The XMC-903 Radome

UNCLASSIFIED

000897

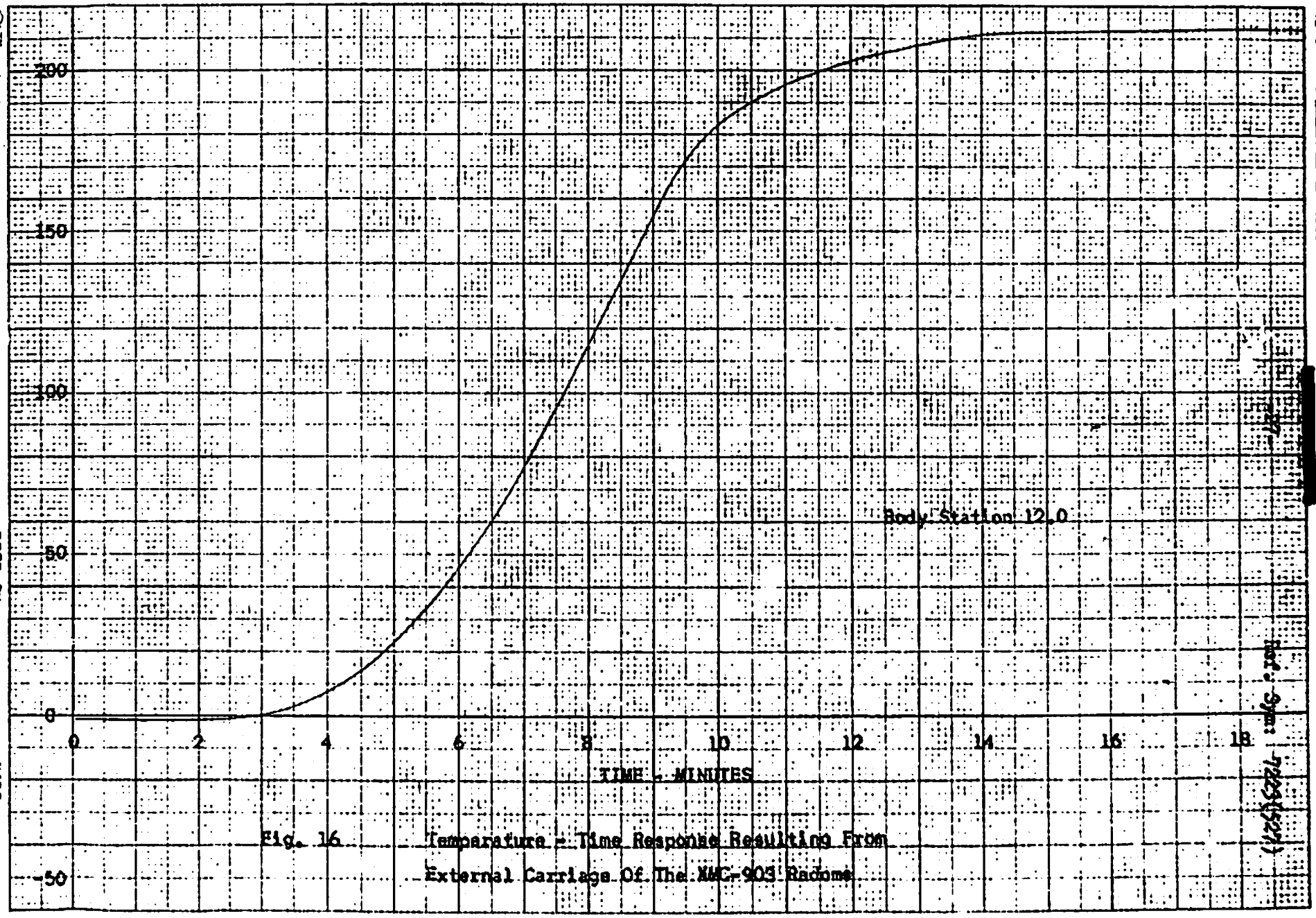

Fig. 16 Temperature - Time Response Resulting From External Carriage Of The XMC-903 Radome

UNCLASSIFIED

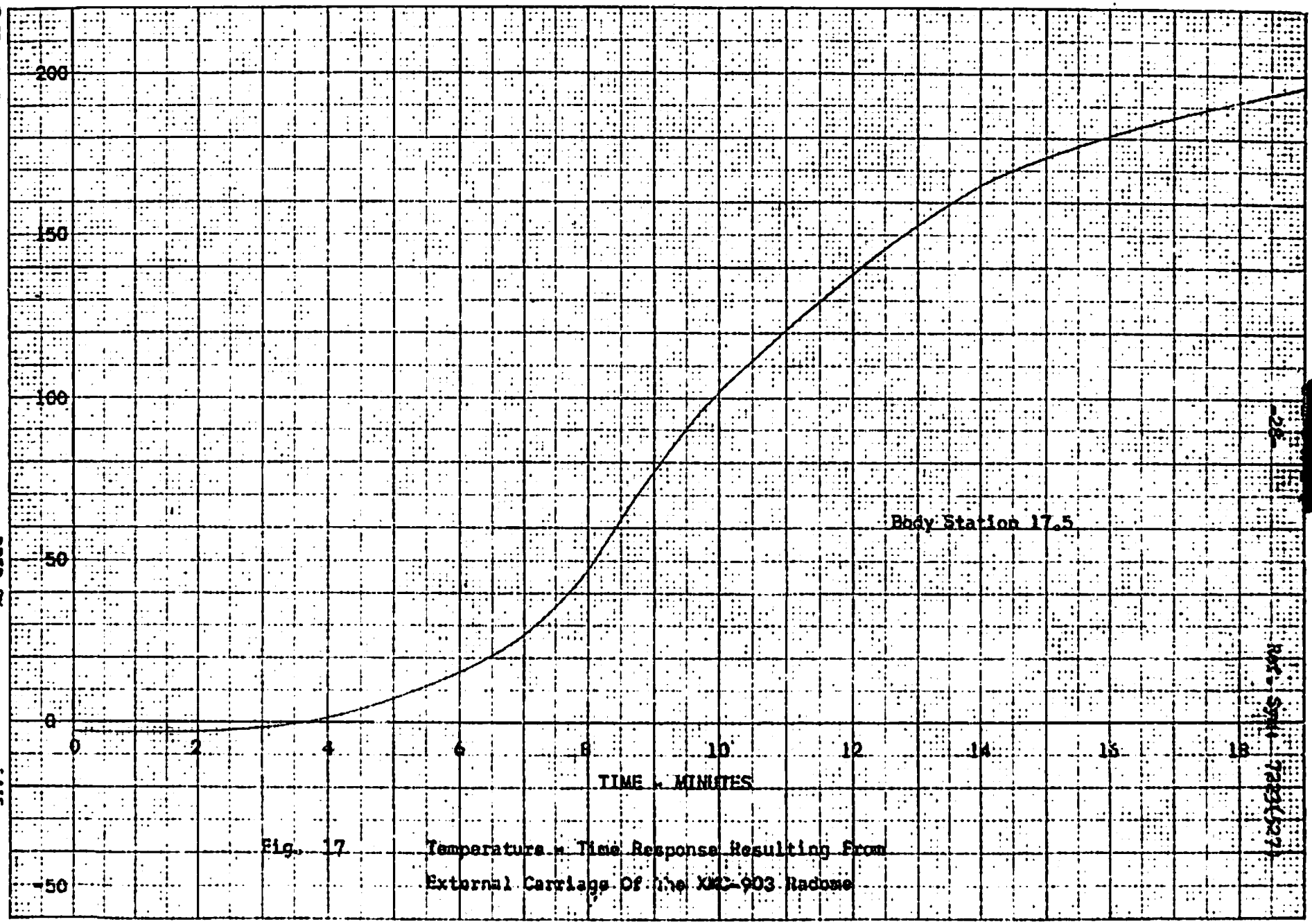

Fig. 17 Temperature - Time Response Resulting From External Carriage Of The XMC-903 Radome

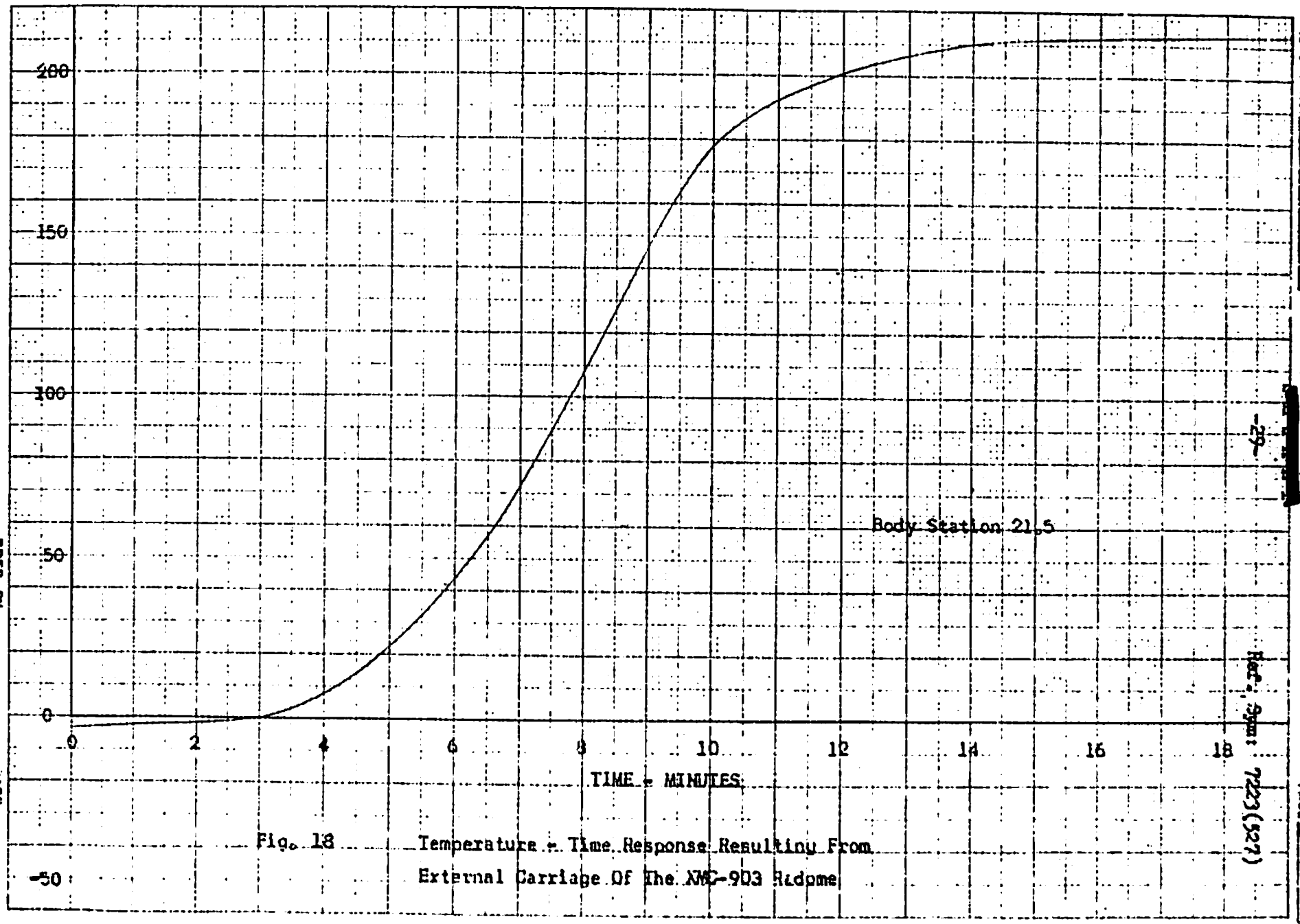

Fig. 18 Temperature - Time Response Resulting From External Carriage Of The XMC-903 Radome

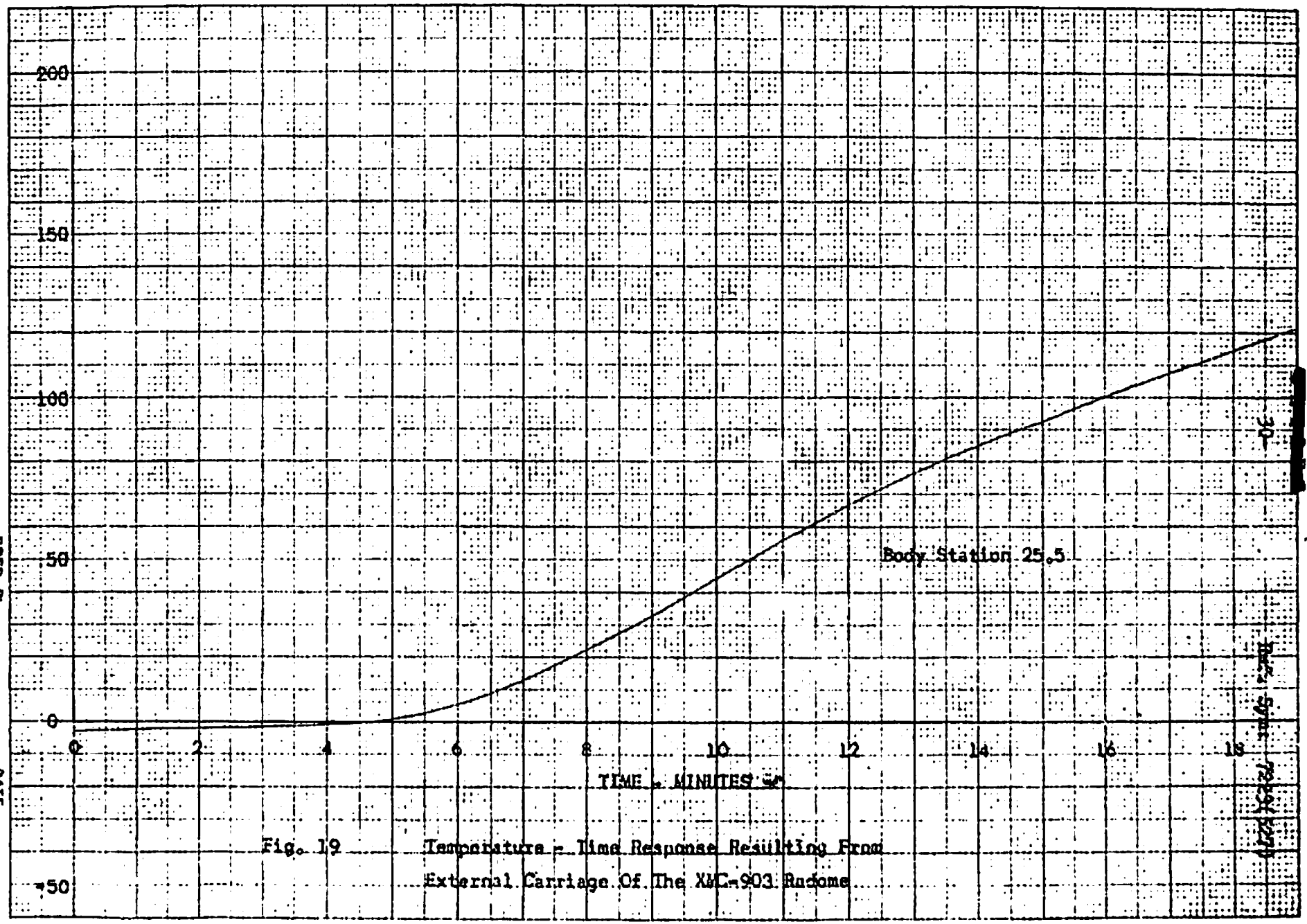

Fig. 19 Temperature - Time Response Resulting From External Carriage Of The XMC-903 Radome

UNCLASSIFIED

[redacted]

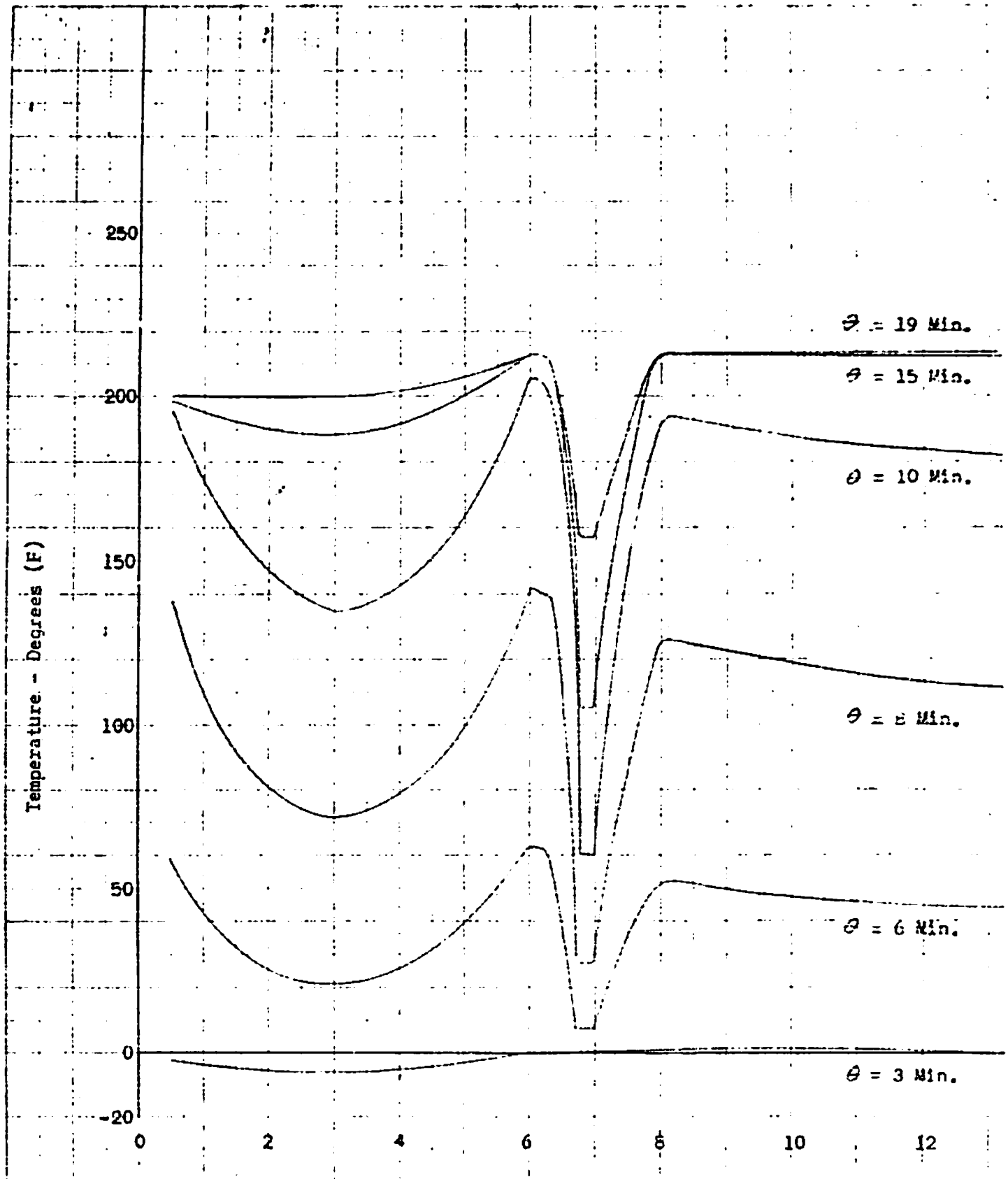

Fig. 20 Temperature Distribution Along the Body at
During External Carriage of the X

UNCLASSIFIED

[redacted]

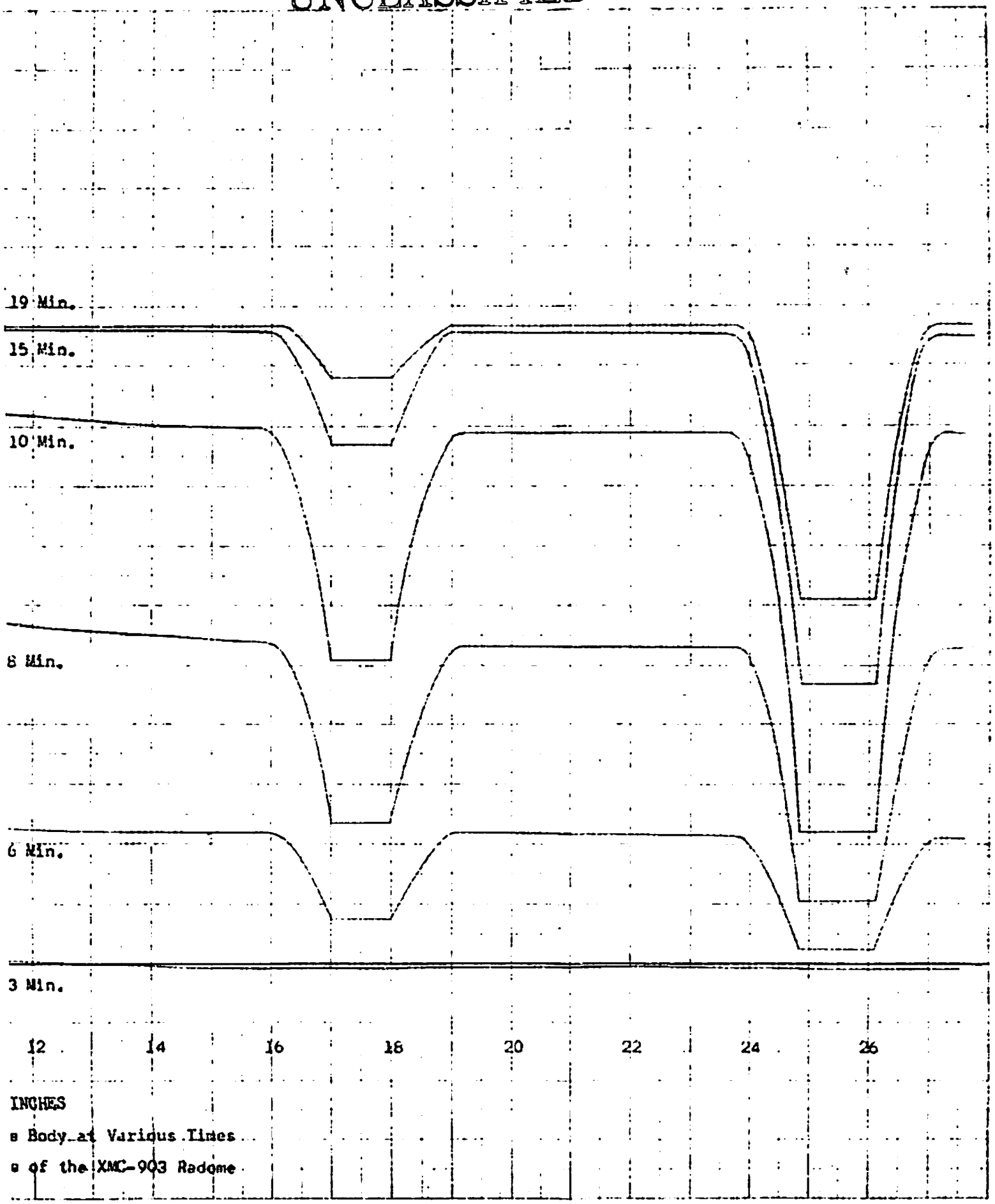

s Body at Various Times
s of the XMC-903 Radome